Journal of Biomolecular NMR, **12:** 51–71, 1998.
KLUWER/ESCOM
© 1998 *Kluwer Academic Publishers. Printed in Belgium.*

Chemical shift as a probe of molecular interfaces: NMR studies of DNA binding by the three amino-terminal zinc finger domains from transcription factor IIIA

Mark P. Foster*, Deborah S. Wuttke**, Karen R. Clemens, Wolfgang Jahnke***, Ishwar Radhakrishnan, Linda Tennant, Martine Reymond, John Chung & Peter E. Wright****
Department of Molecular Biology and Skaggs Institute for Chemical Biology, The Scripps Research Institute, La Jolla, CA 92037, U.S.A.

Received 3 December 1997; Accepted 4 February 1998

Key words: binding, chemical shift, complex, DNA, structure, TFIIIA, Zinc Finger

Abstract

We report the NMR resonance assignments for a macromolecular protein/DNA complex containing the three amino-terminal zinc fingers (92 amino acid residues) of *Xenopus laevis* TFIIIA (termed zf1-3) bound to the physiological DNA target (15 base pairs), and for the free DNA. Comparisons are made of the chemical shifts of protein backbone $^{1}H^{N}$, ^{15}N, $^{13}C^{\alpha}$ and $^{13}C^{\beta}$ and DNA base and sugar protons of the free and bound species. Chemical shift changes are analyzed in the context of the structures of the zf1-3/DNA complex to assess the utility of chemical shift change as a probe of molecular interfaces. Chemical shift perturbations that occur upon binding in the zf1-3/DNA complex do not correspond directly to the structural interface, but rather arise from a number of direct and indirect structural and dynamic effects.

Abbreviations: TFIIIA, *Xenopus laevis* transcription factor IIIA; zf1-3, a protein construct consisting of residues 11–101 of TFIIIA, plus an N-terminal methionine and mutation of Cys^{35} to serine; IPTG, isopropyl-β-D-thiogalactopyranoside; 2D, 3D, two-, three-dimensional NMR spectroscopy; HSQC, heteronuclear single quantum correlation spectroscopy; TOCSY, total correlation spectroscopy; NOE, nuclear Overhauser enhancement.

Introduction

Identifying structural features of biomolecules that are important for conveying their ability to bind ligands and receptors is a primary objective when seeking to understand function in molecular biology, structural biology and drug design. To this end, various techniques (e.g., site-directed mutagenesis, alanine scanning, combinatorial chemistry, SAR) are employed for mapping out the functional regions of proteins, nucleic acids, and small molecules. NMR spectroscopy has long been applied to these problems, with recent studies highlighting the utility of chemical shift analysis for the identification and design of high-affinity ligands for proteins (Shuker et al., 1996; Hajduk et al., 1997), and for mapping intermolecular interfaces (Chen et al., 1993; Gronenborn and Clore, 1993; van Nuland et al., 1993, 1995; Emerson et al., 1995; Grzesiek et al., 1996; Garrett et al., 1997; Scmiedeskamp et al., 1997).

Transcription factor IIIA (TFIIIA) from *Xenopus laevis* oocytes was the first cellular gene-specific transcription factor identified in eukaryotes (Engelke et al., 1980). TFIIIA possesses a tandem repeat of nine zinc finger sequences of the C_2H_2 class and is the protein in which the ubiquitous zinc finger motif was first identified (Ginsberg et al., 1984; Miller et al., 1985;

*Present address: Department of Biochemistry, The Ohio State University, Columbus, OH 43210, U.S.A. **Present address: Department of Chemistry and Biochemistry, University of Colorado, Boulder, CO 80309, U.S.A. ***Present address: Novartis Pharma AG, CH-4002 Basel, Switzerland. ****To whom correspondence should be addressed.

Pieler and Theunissen, 1993). Each zinc finger domain adopts a compact globular structure which consists of a short N-terminal β-strand, followed by a C-terminal α-helix; adjacent fingers are connected by short linkers with highly conserved sequences.

TFIIIA promotes transcription of the 5S RNA gene by RNA polymerase III by binding specifically to an internal control region (ICR) within the 5S RNA gene (Engelke et al., 1980). Remarkably, this versatile factor fulfills a dual role, as it also employs these zinc finger domains to bind specifically to the 5S RNA transcript and functions in RNA storage and transport (Honda and Roeder, 1980; Pelham and Brown, 1980; Guddat et al., 1990). Numerous biochemical studies have been directed towards understanding the structural basis for molecular recognition of DNA and RNA by TFIIIA. These have led to the proposal of conflicting models of the interaction between DNA and the nine zinc fingers of TFIIIA (Fairall et al., 1986; Berg, 1990; Clemens et al., 1992; Hayes and Tullius, 1992).

With the goal of characterizing the solution structure of a TFIIIA/DNA complex, we have obtained NMR assignments of a macromolecular complex containing the three amino-terminal zinc fingers of *X. laevis* TFIIIA (termed zf1-3) bound to the physiological DNA target. The protein binds specifically and with high affinity (5.6 nM) to the C-block element of the ICR in an antiparallel orientation, with finger 1 oriented towards the 3′ end of the binding site and finger 3 towards the 5′ end (Liao et al., 1992). The solution structure of the zf1-3/DNA complex (Foster et al., 1997; Wuttke et al., 1997) reveals structural features that could not have been readily predicted based on the biochemical data and the crystal structures of other zinc finger protein/DNA complexes previously reported (Pavletich and Pabo, 1991, 1993; Fairall et al., 1993; Elrod-Erickson et al., 1996; Houbaviy et al., 1996; Kim and Berg, 1996). In particular, protein dynamics and packing interactions between domains and their associated linkers play an important role in mediating recognition (Foster et al., 1997; Wuttke et al., 1997).

In this study we report the resonance assignments for the zf1-3/DNA complex and free DNA, and compare the chemical shifts determined for zf1-3 (Liao et al., 1994) and its DNA target in their free solution states with those in the complex. Evaluating the chemical shift differences in the context of the structures of the zf1-3/DNA complex allows us to assess the utility of chemical shift analysis as a probe for understanding the mode of interaction of zinc finger proteins with nucleic acids. Our findings suggest that chemical shift changes in macromolecular complexes must be interpreted with care.

Methods

Protein and DNA sequence and numbering

The zf1-3 protein encompasses the three amino-terminal fingers of TFIIIA and retains the N-terminal methionine, plus residues Lys^{11} through Lys^{101}, with a mutation of Cys^{35} to Ser. This protein binds with full specificity and high affinity to the C-block of the 5S RNA gene internal control region (Liao et al., 1992). The 15-base pair oligonucleotide used in this study consists of the experimentally determined minimal 13-base pair binding site from the cognate DNA (Liao et al., 1992) plus two flanking base pairs to compensate for the effects of end-fraying on the NMR spectra.

Sample preparation

The method for the expression of the zf1-3 protein has been described previously (Clemens et al., 1992; Liao et al., 1994; Wuttke et al., 1997). The protein was purified as follows: the urea-solubilized cell extract was diluted four-fold (50 mM potassium phosphate, pH 6.67, 100 μM $ZnCl_2$, 200 mM NaCl, 10 mM DTT and 2 mM NaN_3), eluted from a heparin-Sepharose FPLC column (Pharmacia) with a salt gradient to 1 M NaCl, and purified by preparative reversed-phase HPLC (Waters DELTA-PAK C_4, 300 Å pore size, 15 μm particle size, 30 × 4.7 cm, 100 ml/min, gradient 30–70% B over 40 min: buffer A = 0.1% trifluoroacetic acid (TFA), buffer B = 60% acetonitrile (AcN), 0.1% TFA). Fractions containing pure zf1-3 protein (as judged by isocratic HPLC, Vydac 25 × 0.5 cm C_4 column, 60% buffer B) were pooled, rotovaped for 40 min at room temperature to remove TFA, and lyophilized.

To refold the HPLC-purified zf1-3, the lyophilized protein powder was dissolved in denaturant buffer (50 mM Tris-HCl, pH 7.4 at 25 °C (pH ∼ 6.4 at 70 °C), 50 mM KCl, 100 μM $ZnCl_2$, 150 mM DTT, 6 M Gdn-HCl), incubated for 30 min at 70 °C in a water bath, and allowed to cool to room temperature. The solution was diluted to a Gdn-HCl concentration of 0.2 M and then eluted from a second heparin-Sepharose column with a salt gradient. The fractions containing the folded protein were pooled, concentrated by ultrafiltration (Filtron 1 kDa cutoff membrane, 4 °C), and

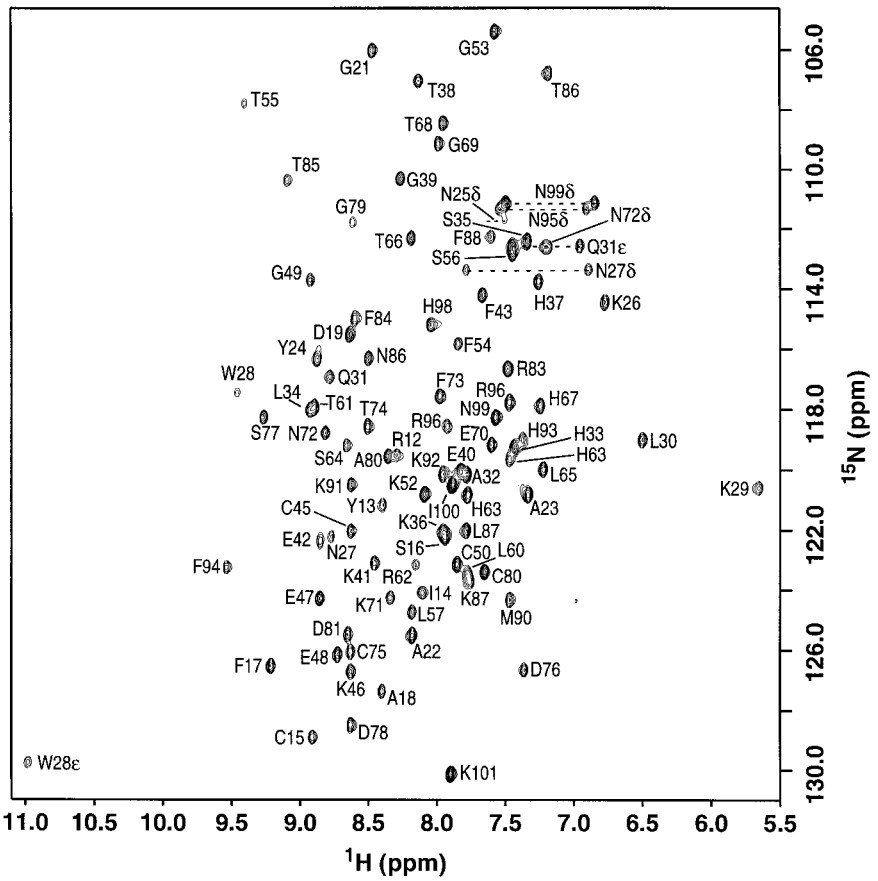

Figure 1. ^{15}N HSQC spectrum of the U-[^{15}N]-zf1-3/DNA complex (750 MHz) with protein amide assignments indicated.

exchanged into NMR buffer (10 mM d_{11}-Tris-HCl, pH 6.7 (adjusted with d_4-acetic acid), 50 mM KCl, 50 μM $ZnCl_2$, 5% D_2O, 5 mM d_{10}-DTT, 2 mM NaN_3). The method for purification of the DNA and preparation of the zf1-3/DNA complex has been described elsewhere (Wuttke et al., 1997). The complex is in slow exchange, with a half-life for dissociation greater than 1 h. All buffers were degassed and saturated with argon before use, and samples were stored under argon at 4 °C.

General NMR methods

For resonance assignments, NMR spectra of the zf1-3/DNA complex were recorded at 310 K on Bruker AMX-500, AMX-600 and DMX-750 spectrometers. Proton chemical shifts were referenced to TMS using the relation $\delta H_2O = 3.18 + (177.6 - T\ (°C))/96.9$ (Orbons et al., 1987). The ^{15}N and ^{13}C chemical shifts were referenced indirectly using the ^{1}H/X frequency ratios of 0.101329118 and 0.251449530 for ammonia and DSS, respectively (Live et al., 1984; Bax and Subramanian, 1986; Wishart et al., 1995). In general, quadrature detection in the indirect dimensions was achieved by the States-TPPI method (States et al., 1982; Kay et al., 1989); in experiments with gradient pulses applied for coherence selection, quadrature was achieved by linear combinations of p- and n-type data (Muhandiram and Kay, 1994). In most cases, the delay for the first time point in the indirect dimension was set for zero evolution or 1/2 ∗ dwell to minimize baseline distortion and ensure absorptive line shapes for aliased peaks (Marion and Bax, 1988; Kay et al., 1989; Bax et al., 1991). NMR data were processed and analyzed using NMR Triad (Tripos Associates Inc.), NMRPipe (Delaglio et al., 1995) or FELIX (MSI Inc.). In general, time-domain data were zero-filled once in the indirect dimensions, and apodized with cosine, Hamming or Lorentzian-to-Gaussian window functions. Linear prediction (LP) was applied where appropriate, using mirror-image LP for indirect heteronuclear di-

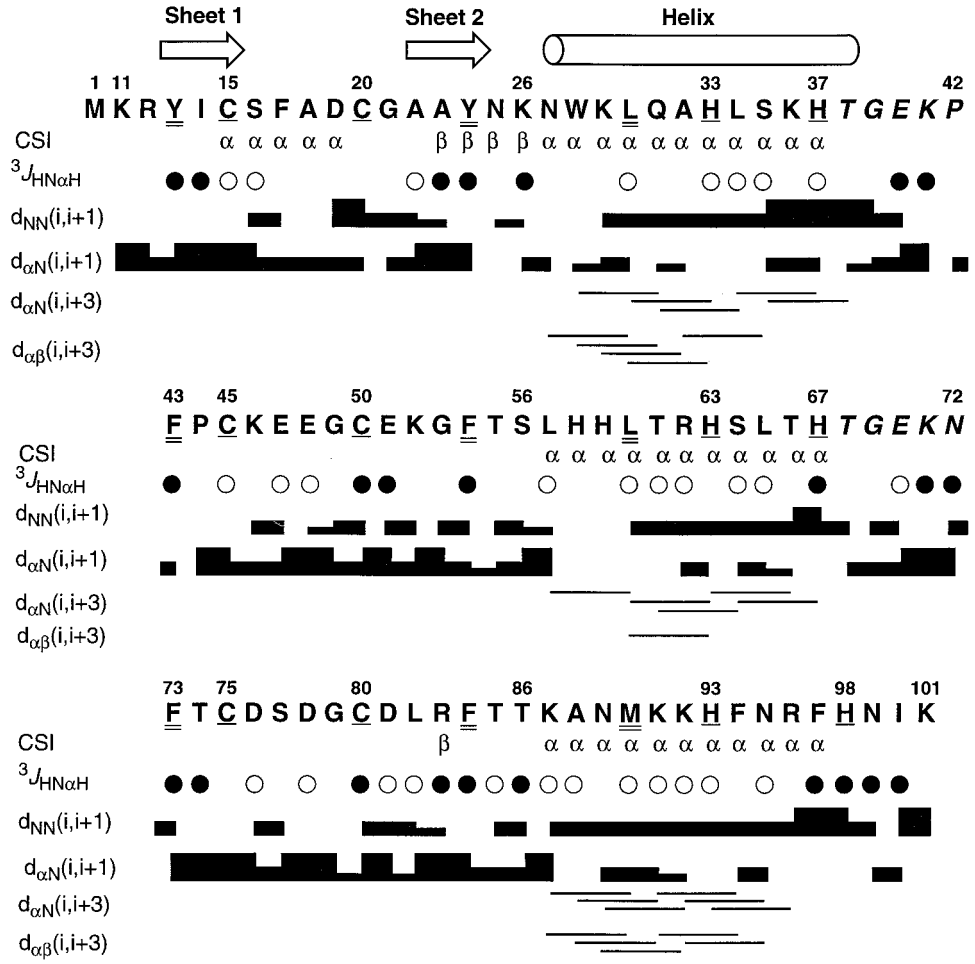

Figure 2. Amino acid sequence of zf1-3 and summary of NMR data that reflect the secondary structural elements in the complex. Conserved zinc ligands (Cys and His) are underlined, conserved hydrophobic residues important for conferring structural integrity are doubly underlined, and the TGEKP and TGEKN linker sequences between the fingers are italicized. In the CSI (chemical shift index) row, α and β designate amino acids that are predicted to possess α-helical and β-sheet structure, respectively, based on backbone chemical shift deviations from random coil (Wishart and Sykes, 1994b). Open circles correspond to small $^3J_{N\alpha}$ couplings (<5 Hz) and filled circles correspond to large couplings (>7.5 Hz). The relative intensity of sequential NOEs is indicated by the width of the bars, and correspond to strong, medium and weak cross peaks. The presence of short-range (i, i+3) $d_{\alpha N}$ and $d_{\alpha\beta}$ NOEs is indicated by lines.

mensions acquired with constant-time evolution (Zhu and Bax, 1992). Time-domain data acquired with digital filters (on the Bruker DMX-750) were processed either by application of a large linear phase correction after apodization and Fourier transformation, or by using the appropriate DMX parameters for 'bruk2pipe' in the NMRPipe software (Delaglio et al., 1995). Table 1 contains a listing of the NMR experiments and relevant parameters from which resonance assignments were extracted for the zf1-3/DNA complex and for the free DNA.

The ^{15}N-separated TOCSY and NOESY (Bax et al., 1990c), constant-time HNCA and HN(CO)CA (Grzesiek and Bax, 1992b) spectra were acquired without gradients, using spin-lock purge pulses for water suppression (Messerle et al., 1989). The 3D CBCA(CO)NH (Grzesiek and Bax, 1992b) and HBHA(CBCACO)NH (Grzesiek and Bax, 1993a) data sets were obtained without gradients, using a pair of x/y spin-locks to scramble the water signal while magnetization was antiphase for ^{13}CO and ^{15}N, immediately preceding the ^{15}N constant-time evolution period. The ^{15}N HSQC (Bodenhausen and Ruben, 1980) and ^{15}N HSQC-NOESY spectra obtained at 750 MHz were acquired with water flip-back pulses (Grzesiek and Bax, 1993b), sensitivity enhancement (Cavanagh

Table 1. Pulse sequences used ot assign the zf1-3/DNA complex and free DNA

Experiment	SF	Time domain sizes (points)			Spectral widths (Hz)			τ(ms)
		t_1	t_2	t_3	ω_1	ω_2	ω_3	
U-[^{15}N]-zf1-3/DNA complex, 95:5 H_2O/D_2O								
^{15}N HSQC	750	512 (H)	128 (N)		6009.6	3030.3		
^{15}N NOESY-HSQC	600	512 (H)	128 (H)	32 (N)	8402.0	6601.5	2432.7	120
^{15}N TOCSY-HSQC	600	512 (H)	128 (H)	32 (N)	8402.0	6601.5	2432.7	62
^{15}N NOESY-HSQC	750	512 (H)	128 (H)	32 (N)	6009.61	7518.8	2283.1	31
HNHA	500	1024 (H)	104 (H)	32 (N)	7042.3	5000.0	1500.2	
HNHB	500	512 (H)	64 (H)	32 (N)	4032.3	5000.0	1500.2	
JR-NOESY	600	8192 (H)	512 (H)		15151.5	15151.5		120
U-[^{15}N/^{13}C]-zf1-3/DNA complex, 95:5 H_2O/D_2O								
HNCA	500	2048 (H)	92 (N)	32 (C)	6024.1	1470.6	2388.9	
HN(CO)CA	500	2048 (H)	58 (N)	46 (C)	6024.1	1470.6	2388.9	
HNCO	500	1024 (H)	64 (N)	32 (C)	6024.1	1470.6	1515.2	
C(CO)NH-TOCSY	500	512 (H)	64 (C)	32 (N)	4032.3	8928.6	1515.2	21
CBCA(CO)NH	600	1024 (H)	56 (C)	24 (N)	9615.4	8598.4	1702.4	
HBHA(CBCACO)NH	600	1024 (H)	85 (H)	27 (N)	9615.4	2570.7	1702.4	
U-[^{15}N/^{13}C]-zf1-3/DNA complex, 99% D_2O								
^{13}C HSQC	600	1024 (H)	128 (C)		9615.4	12077.3		
^{13}C HSQC (AR)	600	1024 (H)	81 (C)		9615.4	4527.0		
HCCH-COSY	600	512 (H)	128 (H)	22 (C)	6024.1	2998.5	4111.8	
HCCH-TOCSY	600	512 (H)	128 (H)	22 (C)	6024.1	3000.3	4111.8	19.6
^{13}C NOESY-HSQC	600	512 (H)	128 (H)	27 (C)	6024.1	2999.4	4111.8	80
^{13}C NOESY-HSQC	750	512 (H)	128 (H)	27 (C)	8680.6	7575.8	5140.2	80
HACAHB-COSY	750	512 (H)	55 (H)	24 (C)	6009.6	4882.8	3583.4	
C′-Cγ diff. HSQC	500	1024 (H)	256 (C)		6024.1	10000.0		
C′-N diff. HSQC	500	1024 (H)	256 (C)		6024.1	10000.0		
^{13}C-edited, ^{13}C/^{15}N-filtered NOESY	750	1024 (H)	256 (H)	19 (C)	12500.0	6756.8	7575.8	120
NOESY (^{13}C-decoupled)	750	4096	512		12500.0	7518.8		30, 60, 120
^{13}C/^{15}N-filtered NOESY	750	4096	512		12500.0	7518.8		30, 60, 120
^{13}C/^{15}N-filtered TOCSY	750	4096	480		12500.0	7518.8		41
Free DNA, 99% D_2O								
NOESY	750	4096	512		12500.0	7518.8		30, 60, 120
TOCSY	750	4096	512		12500.0	7518.8		41

SF, spectrometer frequency (MHz) for protons; τ, mixing time; time-domain sizes are in complex points, and the corresponding nucleus (^{1}H, ^{13}C or ^{15}N) is indicated.

and Rance, 1993) and gradient pulses for coherence selection (Kay, 1995). The 3D HNHA spectrum (Vuister and Bax, 1993) was recorded with pulsed field gradients for artifact suppression (Bax and Pochapsky, 1992) and the HNHB spectrum (Archer et al., 1991) with water flip-back pulses (Grzsiek and Bax, 1993b; Kay et al., 1994), sensitivity enhancement (Palmer et al., 1991) and gradient pulses for coherence selection. The C(CO)NH-TOCSY (Grzesiek and Bax, 1992a) was acquired with gradient pulses for coherence selection, and three cycles of DIPSI-3 mixing at an rf field strength of 7.8 kHz (21 ms mixing), with the goal of seeing correlations from the longer side-chains (e.g., lysine C^ϵ) to the backbone NH of the following residue in the sequence.

Doubly ^{13}C/^{15}N-filtered NOESY and TOCSY spectra (Otting and Wüthrich, 1990; Ikura and Bax, 1992; Burgering et al., 1993; Slijper et al., 1996) employed spin-echo difference pulses for filtering, while storing only the sum data sets. Magnetization from residual amide protons was filtered in a time-shared manner with respect to ^{1}H-^{13}C filtering (Burgering et

Table 2. zf1-3 shifts in complex with DNA, 310 K[a]

Res.	N H^N	C^α H^α	CO	C^β H^β [b]	C^γ H^γ	C^δ H^δ	Others
Met[1]		55.4/3.94	NA	34.4/2.10	31.4/2.58		C^ϵ 16.9/2.14
Lys[11]		56.2/4.26	175.3	32.9/1.65,1.47	25.6/1.43,1.13	29.0/1.54	C^ϵ 42.0/2.95
Arg[12]	119.8/8.25	56.1/4.30	175.5	31.3/*1.55*,1.61	27.1/1.39,1.29	43.4/3.08	
Tyr[13]	121.5/8.41	58.0/4.56	174.3	37.5/*2.95*,2.80	132.9/7.04 C^ϵ 117.9/6.88		
Ile[14]	124.2/8.10	60.2/4.69	175.1	40.9/1.70	27.6/1.43,0.99	13.6/0.84	$C^{\gamma 2}$ 17.1/0.92
Cys[15]	129.1/8.92	62.2/4.31	176.8	30.0/3.20,*2.97*			
Ser[16]	122.4/7.94	58.5/4.51	174.9	63.8/4.06,3.91			
Phe[17]	126.7/9.20	60.0/4.13	176.4	38.6/*2.72*,2.65		131.7/7.17	C^ϵ 131.8/7.31,7.26
Ala[18]	127.6/8.39	54.0/4.02	177.7	18.4/1.35			
Asp[19]	115.7/8.62	55.0/4.37	174.7	39.8/2.87,2.84			
Cys[20]	121.1/7.79	61.1/4.55	176.4	29.5/3.27,3.00			
Gly[21]	106.3/8.44	45.5/3.94	174.1				$H^{\alpha+}$ 3.98
Ala[22]	125.9/8.19	54.0/3.92	175.1	19.0/0.87			
Ala[23]	121.1/7.33	50.8/5.06	175.8	23.0/1.19			
Tyr[24]	116.6/8.87	56.7/4.97	175.3	45.2/3.12,*2.69*		133.6/6.98	C^ϵ 117.5/6.50
Asn[25]	116.4/8.83	52.2/5.40	175.3	38.8/3.58,2.86			$N^{\delta 2}$ 111.8/7.70,7.51
Lys[26]	114.6/6.80	53.7/4.59	175.4	38.9/*0.92*,1.97	25.0/1.70,1.58	29.0/2.17,1.85	C^ϵ 42.2/3.01,2.97
Asn[27]	122.4/8.78	56.2/3.86	178.8	38.7/2.79,*2.56*			$N^{\delta 2}$ 113.5/7.78,6.88
Trp[28]	117.6/9.41	59.9/4.37	178.3	26.5/3.53,3.32			$C^{\delta 1}$ 128.5/7.64
							$N^{\epsilon 1}$ 130.1/10.97
							$C^{\zeta 2}$ 115.0/7.69
							$C^{\eta 2}$ 123.8/6.06
							$C^{\zeta 3}$ 122.5/6.98
							$C^{\epsilon 3}$ 120.8/7.35
Lys[29]	120.7/5.67	58.2/3.00	178.1	32.7/1.29,1.18	23.7/−0.63,−0.95	1.81,1.69	C^ϵ 42.0/2.93,2.56
Leu[30]	119.3/6.54	57.5/3.97	177.9	40.7/2.21,*1.50*	27.5/1.75	$C^{\delta x}$ 26.0/1.20	$C^{\delta Y}$ 21.9/1.17
Gln[31]	117.1/8.76	58.7/4.00	179.2	27.6/2.29,*2.16*	33.2/2.51		$N^{\epsilon 2}$ 112.5/7.46,6.93
Ala[32]	120.4/7.79	55.5/4.28	180.0	18.4/1.67			
His[33]	119.4/7.47	60.0/4.35	177.1	28.2/*3.62*,3.37		$C^{\delta 2}$ 125.9/7.22	$C^{\epsilon 1}$ 138.7/7.88
Leu[34]	118.1/8.93	58.6/4.03	179.4	42.0/*2.12*,1.74	27.2/2.20	25.8/1.15	$C^{\epsilon Y}$ 25.1/1.47
Ser[35]	112.7/7.37	61.9/4.45	176.2	63.5/3.94,*4.04*			
Lys[36]	122.3/7.95	58.8/3.98	178.3	31.4/1.49	24.5/1.37,1.25	28.8/1.70,1.54	C^ϵ 41.5/2.95
His[37]	114.0/7.29	56.5/4.33	177.3	28.8/*2.77*,2.08		$C^{\epsilon 2}$ 128.5/6.54	$C^{\epsilon 1}$ 138.9/7.93
Thr[38]	107.3/8.12	62.5/4.32	176.6	70.5/4.43	21.2/1.40		
Gly[39]	110.5/8.26	45.6/3.76	174.5				$H^{\alpha+}$ 4.16
Glu[40]	120.2/7.83	55.9/4.26	176.0	30.4/1.86,1.82	36.0/2.17,2.07		
Lys[41]	123.3/8.44	51.9/4.63 b	32.7/*1.69*,1.40	28.4/1.17,1.13	28.8/1.41,1.12		C^ϵ 42.1/2.84,2.75
Pro[42]	63.8/4.29	175.4	31.7/2.12,1.45	26.8/2.18,2.13	51.0/3.81,3.73		
Phe[43]	114.4/7.68	55.2/5.07	NA	39.6/3.05,*2.75*		131.4/7.06	C^ϵ 131.0 7.38,7.46
Pro[44]		62.4/4.84	175.6	32.4/2.26,1.92	26.9/2.03,2.07	50.6/3.79,3.49	
Cys[45]	122.4/8.64	60.8/4.51	176.8	30.1/3.22,*2.80*			
Lys[46]	126.7/8.59	55.7/4.55	177.3	31.9/2.13,*1.82*	24.5/1.57,1.53	28.4/1.74	C^ϵ 41.9/3.08
Glu[47]	124.4/8.86	56.7/4.05	177.5	29.2/1.62,1.57	34.8/1.64,1.40		
Glu[48]	126.4/8.70	58.4/4.02	178.1	29.1/2.02,1.99	36.1/2.29		
Gly[49]	113.7/8.90	45.3/3.76	173.2				$H^{\alpha+}$ 4.21
Cys[50]	123.3/7.87	60.5/4.59	175.4	30.4/3.24,*2.75*			
Glu[51]	122.5/8.83	56.0/4.62	176.4	29.3/*2.32*,1.92	36.6/2.20,2.25		
Lys[52]	121.0/8.11	56.2/4.25	175.3	34.0/1.41,*1.56*	25.5/1.53,1.63	28.9/1.68,1.73	C^ϵ 42.1/3.11

Table 2 continued.

Res.	N H^N	C^α H^α	CO	C^β H^β	C^γ H^γ	C^δ H^δ	Others
Gly[53]	105.7/7.57	44.7/3.50	171.3				$H^{\alpha+}$ 4.61
Phe[54]	116.0/7.88	57.9/5.13	176.0	43.9/3.69,*3.00*		132.1/7.58	C^ϵ 130.5/6.87
							C^ζ 129.6/6.62
Thr[55]	108.0/9.37	62.5/4.53	173.7	69.1/4.76	22.7/1.50		
Ser[56]	112.9/7.46	56.0/4.52	173.0	66.6/*3.85*,3.70			
Leu[57]	125.4/8.19	57.3/3.40	NA	40.8/1.43,*1.11*	26.6/1.33	25.2/0.89	$C^{\delta Y}$ 23.0/0.95
His[58]	NA	59.9/4.11	NA	30.1/3.13,2.77		$H^{\delta 2}$ 7.20	NA
His[59]	NA	57.6/NA	173.2	NA		NA	$H^{\epsilon 1}$ 8.64
Leu[60]	123.8/7.78	58.5/3.78	177.9	40.5/2.19,*1.74*	27.5/1.70	26.2/1.12	$C^{\delta Y}$ 22.3/1.20
Thr[61]	118.1/8.89	66.8/3.84	177.3	68.2/4.16	21.6/1.22		
Arg[62]	123.3/8.14	59.2/4.00	178.5	31.6/1.32,1.78	25.1/1.70,1.47	44.7/3.01,2.87	
His[63]	119.8/7.49	58.7/4.60	178.3	28.2/*2.57*,3.24		$C^{\delta 2}$ 127.2/7.17	$C^{\epsilon 1}$ 137.5/7.36
Ser[64]	119.3/8.67	62.8/4.22	175.8	62.7/4.14			
Leu[65]	120.3/7.24	57.1/4.47	180.7	41.6/*1.93*,1.70	26.9/1.98	25.8/1.11	$C^{\delta Y}$ 22.9/1.00
Thr[66]	112.6/8.19	64.4/4.25	176.2	68.9/4.11	21.3/1.43		
His[67]	118.1/7.27	57.0/4.70	176.6	28.6/3.27,*3.37*		$C^{\delta 2}$ 127.0/6.63	$C^{\epsilon 1}$ 139.6/8.08
Thr[68]	108.8/7.95	62.8/4.41	176.9	69.7/4.41	21.5/1.31		
Gly[69]	109.3/8.01	46.1/3.88	174.5				$H^{\alpha+}$ 4.04
Glu[70]	119.4/7.61	57.6/4.03	176.4	30.4/1.94,*1.89*	36.6/2.18,2.29		
Lys[71]	124.3/8.31	55.4/4.45	175.8	33.5/*1.67*,1.33	24.5/1.35,1.09	29.6/1.46	C^ϵ 42.1/2.90 2.86
Asn[72]	119.0/8.79	53.8/4.66	174.7	39.5/2.49,*2.22*			$N^{\delta 2}$ 112.8/$Q^{\delta 2}$ 7.18
Phe[73]	117.6/8.01	58.0/4.78	175.3	40.0/2.88,*2.75*		125.9/7.19	C^ϵ 132.1/7.48
Thr[74]	118.6/8.50	61.1/4.88	173.7	69.9/4.19	21.9/1.31		
Cys[75]	126.0/8.62	61.7/4.35	175.8	29.6/3.14			
Asp[76]	126.8/7.39	56.0/4.67	177.3	42.2/2.63,2.25			
Ser[77]	118.5/9.25	58.9/4.39	176.0	62.9/3.43,*3.07*			
Asp[78]	128.6/8.61	56.2/4.47	177.5	40.8/2.69,2.67			
Gly[79]	111.9/8.61	45.4/3.88	173.0				$H^{\alpha+}$ 4.10
Cys[80]	123.6/7.67	59.4/4.58	174.5	30.9/3.26,*2.75*			
Asp[81]	125.9/8.63	53.7/4.93	176.2	41.5/2.80,*2.64*			
Leu[82]	122.2/7.79	56.2/4.05	175.2	43.0/*1.55*,1.04	27.5/1.78	26.0/0.83	$C^{\delta Y}$ 23.0/0.81
Arg[83]	116.8/7.46	53.9/5.17	174.7	34.0/*1.67*,1.37	27.8/1.49,1.67	43.5/3.23,3.17	
Phe[84]	115.4/8.61	57.0/5.18	176.8	44.7/*2.74*,3.46		130.7/7.32	C^ϵ 130.3/7.01
							C^ζ 129.5/5.81
Thr[85]	110.9/9.13	64.3/4.61	176.4	69.9/4.52	24.2/1.60		
Thr[86]	106.9/7.20	58.5/4.48	177.3	72.7/4.26	20.6/1.10		
Lys[87]	124.1/7.78	59.4/3.18	178.3	31.8/*1.57*,1.21	24.9/1.34,1.29	29.2/1.84,1.75	C^ϵ 42.1/3.02,2.97
Ala[88]	119.8/8.32	54.7/4.12	180.7	18.8/1.40			
Asn[89]	118.6/7.94	55.5/4.52	178.1	36.9/3.05			
Met[90]	124.5/7.49	60.0/2.46	177.7	29.5/1.62,1.71	33.5/2.40		C^ϵ 16.9/2.19
Lys[91]	120.7/8.63	59.1/4.00	178.6	32.0/1.93	24.8/1.61,1.48	28.7/1.66	C^ϵ 41.8/2.92
Lys[92]	120.5/7.98	60.0/4.15	179.6	32.4/2.01	24.5/1.45,1.77	29.7/1.98,1.83	C^ϵ 41.6/3.06
His[93]	119.3/7.39	59.6/4.62	176.9	28.0/*3.39*,3.27		7.63	$C^{\epsilon 1}$ 138.2/7.51
Phe[94]	123.4/9.54	61.9/3.96	177.9	39.6/3.50		132.1/7.46	C^ϵ 129.3/7.27
							C^ζ 129.5/7.42
Asn[95]	116.7/8.54	55.5/4.58	176.4	38.3/*2.97*,2.93			$N^{\delta 2}$ 111.6/7.56,6.90
Arg[96]	117.8/7.49	58.7/4.02	177.7	31.3/1.80,1.39	27.5/1.50,1.67	43.9/3.23,3.10	

Table 2 continued.

Res.	N H^N	C^α H^α	CO	C^β H^β	C^γ H^γ	C^δ H^δ	Others
Phe[97]	112.6/7.64	59.7/4.32	176.2	40.4/2.32,*1.35*		131.9/7.15	C^ϵ 131.2/7.57
							C^ζ 129.5/7.42
His[98]	115.3/8.03	53.6/5.04	174.1	28.4/2.76,*1.69*		$C^{\delta 2}$ 128.5/6.61	$C^{\epsilon 1}$ 138.7/8.00
Asn[99]	118.5/7.57	52.7/4.80	174.5	39.2/*2.98*,2.65			$N^{\delta 2}$ 111.4/7.50,6.82
Ile[100]	120.5/7.86	61.1/4.18	175.3	38.6/1.90	27.1/1.44,1.15	12.7/0.87	$C^{\gamma 2}$ 17.5/0.91
Lys[101]	130.2/7.87	57.6/4.21	NA	33.8/1.74,1.85	24.5/1.41	28.7/1.70	C^ϵ 42.1/3.03

a. Resonance assignments for X/H pairs are indicated with the heteronuclear assignment first, followed by the proton assignment(s). Unassigned resonances are indicated by NA.
b. In stereospecifically assigned β-methylene pairs, the pro-R proton is italicized.

Table 3. ^{1}H shifts of free DNA, at 310 K

Nucleotide	H1′	H2′ H2″	H3′	H4′	H2/H5/H7	H6/H8
T1	6.05	2.12,2.50	4.72	4.06	1.68	7.49
T2	5.83	2.11,2.40	4.84	4.17	1.81	7.46
G3	5.65	2.68,2.79	4.98	4.36		7.92
G4	5.72	2.62,2.78	5.00	4.40		7.77
A5	6.22	2.58,2.91	4.99	4.42	(H2) 7.78	8.13
T6	5.71	1.90,2.31	4.83	4.24	1.34	7.02
G7	5.63	2.56,2.70	4.95	4.32		7.76
G8	5.69	2.48,2.69	4.94	4.34		7.65
G9	5.50	2.46,2.66	4.94	4.30		7.60
A10	6.00	2.56,2.84	5.02	4.39	(H2) 7.63	8.00
G11	5.48	2.52,2.67	4.97	4.35		7.63
A12	6.21	2.62,2.87	4.99	4.44	(H2) 7.85	8.08
C13	5.85	1.96,2.38	4.78	4.14	5.21	7.25
C14	5.75	1.97,2.34	4.82	4.10	5.59	7.43
G15	6.19	2.40,2.63	4.68	4.18		7.95
C16	5.81	1.86,2.38	4.69	4.07	5.89	7.58
G17	5.68	2.71,2.80	4.98	4.22		7.94
G18	6.05	2.56,2.81	4.93	4.43		7.74
T19	6.05	2.21,2.56	4.88	4.25	1.35	7.26
C20	6.00	2.14,2.14	4.76	4.15	5.61	7.59
T21	6.03	2.21,2.54	4.87	4.22	1.64	7.44
C22	5.93	2.22,2.47	4.82	4.20	5.67	7.56
C23	5.86	2.11,2.44	4.79	4.15	5.56	7.48
C24	5.50	2.12,2.41	4.83	4.11	5.63	7.49
A25	6.26	2.69,2.94	5.00	4.40	(H2) 7.62	8.29
T26	5.89	2.08,2.47	4.85	4.19	1.43	7.17
C27	5.95	2.08,2.41	4.80	4.14	5.61	7.51
C28	5.52	1.80,2.17	4.77	4.02	5.66	7.40
A29	6.00	2.62,2.71	4.97	4.31	(H2) 7.72	8.11
A30	6.22	2.42,2.59	4.99	4.23	(H2) 7.72	8.13

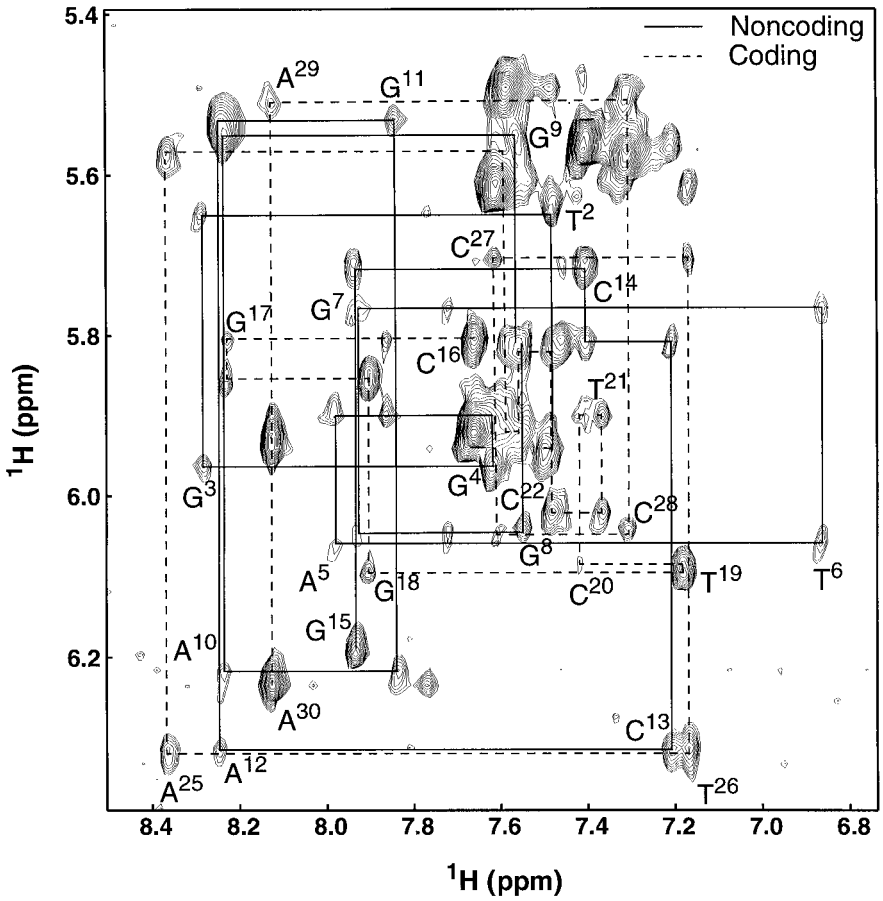

Figure 3. Fingerprint region of the 750 MHz $^{13}C/^{15}N$ (ω_1,ω_2)-filtered NOESY spectrum of the U-[^{15}N,^{13}C]-zf1-3/DNA complex illustrating a 'NOESY walk' with the indicated DNA ^{1}H assignments.

al., 1993; Slijper et al., 1996), using a singly tuned spin-echo difference filter set for a one-bond proton-nitrogen coupling constant, $^{1}J_{NH}$, of 90 Hz. For the NOESY, a single ^{1}H-^{13}C filter was applied in ω_1 (tuned to a $^{1}J_{CH}$ of 125 Hz), with doubly tuned ^{1}H-^{13}C filters employed in ω_2 ($^{1}J_{CH}$ of 125 and 160 Hz). The TOCSY spectrum employed a doubly tuned spin-echo difference $^{13}C/^{15}N$ filter only along ω_2.

Assignment of protein resonances was achieved in a semi automated fashion with the assistance of a series of bookkeeping and strip-manipulation tools written in SPL (SYBYL Programming Language; Tripos Inc.), macros written in-house and interfacing with NMR Triad, and with the tools in the GENXPK suite of programs (G.P. Gippert, unpublished). Finally, for comparison with the free zf1-3 protein, amide ^{15}N and $^{1}H^{N}$ backbone assignments (supplementary material) were obtained at 300 K by transferring assignments from the complex spectrum via a temperature titration.

Analysis of chemical shift changes

Chemical shifts of the zf1-3/DNA complex were compared with the resonance assignments of the individual components free in solution. Systematic differences in chemical shift referencing of resonances for the free and DNA-complexed zf1-3 protein were corrected for by subtracting the trimmed mean chemical shift difference for that nucleus from the observed chemical shift difference. Normalized weighted average chemical shift differences (Δ_{av}/Δ_{max}) for zf1-3 amide ^{1}H and ^{15}N chemical shifts upon DNA binding were calculated using $\Delta_{av}(NH) = [(\Delta H^2 + (\Delta N/5)^2)/2]^{1/2}$, where ΔH and ΔN are the differences between the free and bound chemical shifts (Garrett et al., 1997). Backbone C^{α} and side-chain C^{β} resonances were included in $\Delta_{av}(NHC^{\alpha}C^{\beta}) = [(\Delta H^2 + (\Delta N/5)^2 + (\Delta C^{\alpha}/2)^2 + (\Delta C^{\beta}/2)^2)/4]^{1/2}$ (Grzesiek et al., 1996), except for glycine and proline residues, in which

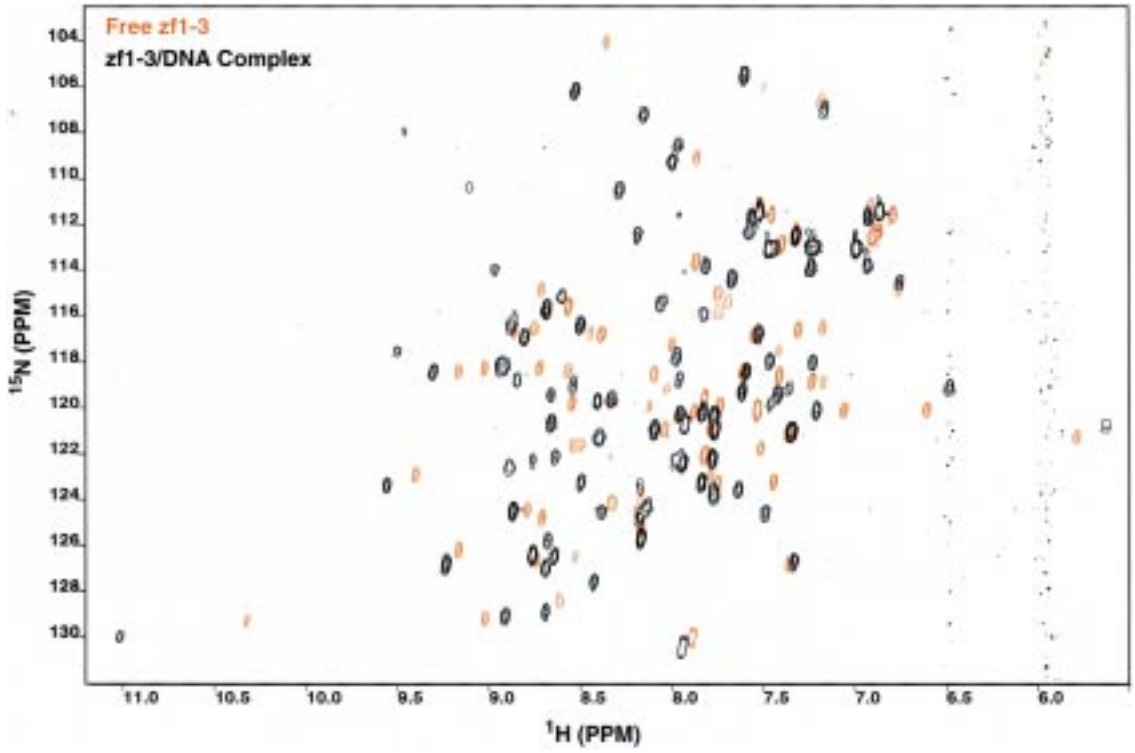

Figure 4. Comparison of ^{15}N HSQC spectra (500 MHz, 300 K) of uniformly labeled zf1-3 protein free (orange) and complexed to DNA (black).

cases δ_{av} was calculated as $[(\Delta H^2 + (\Delta N/5)^2 + (\Delta C^{\alpha}/2)^2)/3]^{1/2}$ and $[((\Delta C^{\alpha}/2)^2 + (\Delta C^{\beta}/2)^2)/2]^{1/2}$, respectively.

Normalized weighted average shift differences were color-mapped onto a tube representation of the mean structure of zf1-3 using the GRASP software (Nicholls et al., 1991). Color ramps were selected with the low, middle and high points of the color maps as the trimmed mean value for Δ_{av} (0.199 for HN and 0.286 for $HNC^{\alpha}C^{\beta}$), one standard deviation from the corresponding trimmed mean (0.321 for HN and 0.426 for $HNC^{\alpha}C^{\beta}$), and unity (Δ_{max}). This approach permits the identification of statistically significant chemical shift perturbations. The low, middle and high values for the surface color map of the magnitude of ^{1}H chemical shift changes for the DNA were 0, 0.03 and 0.06 ppm, respectively.

Results

Assignments

Protein assignments

Protein ^{1}H, ^{13}C and ^{15}N resonance assignments (Table 2) were extracted primarily from heteronuclear-edited NMR spectra at 310 K (see Table 1 for details). Sequence-specific backbone H^{N}, N and C^{α} assignments were derived from analysis of 3D HNCA and HN(CO)CA spectra; CBCA(CO)NH spectra provided confirmation of these assignments as well as C^{β} assignments. Backbone H^{α} and side-chain H^{β} assignments were derived from HBHA(CBCACO)NH (Grzesiek and Bax, 1993a) and 3D ^{15}N-separated TOCSY spectra. The complete assignment of aliphatic side-chain resonances proceeded from an examination of 3D ^{15}N-separated TOCSY, HCCH-COSY, HCCH-TOCSY (Bax et al., 1990a,b; Kay et al., 1990;) and C(CO)NH-TOCSY spectra. Aromatic ^{1}H and ^{13}C resonances were assigned from 2D ^{13}C-decoupled NOESY, ^{13}C-separated HSQC-NOESY, and aromatic carbon HSQC and CT-HSQC spectra (Vuister and Bax, 1992). Backbone carbonyl assignments were ob-

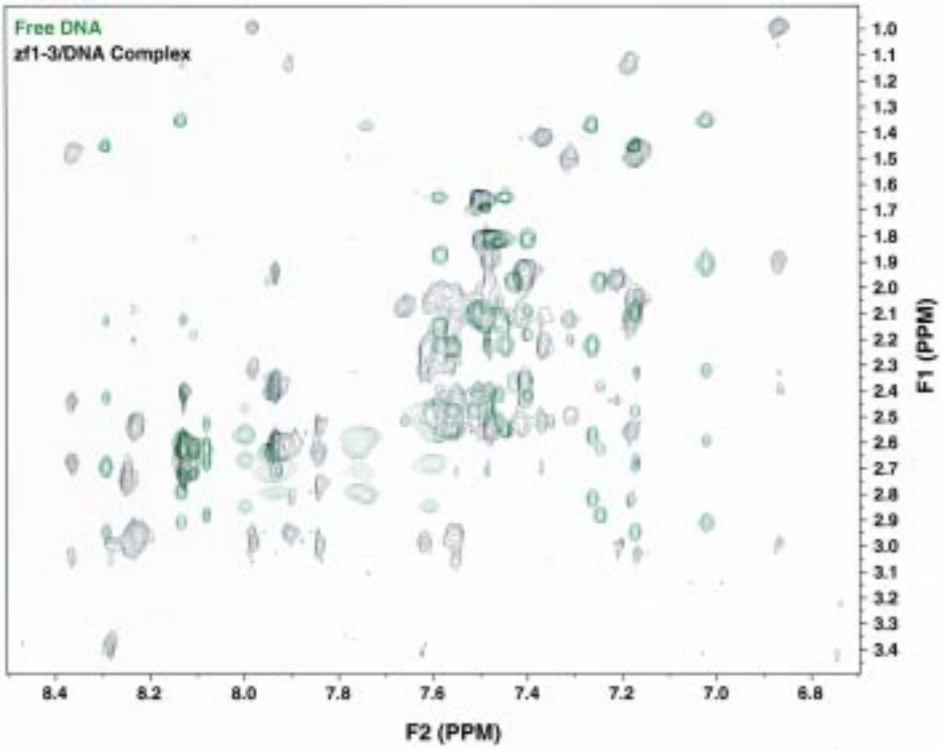

Figure 5. Comparison of the 2D NOESY spectrum (750 MHz, 310 K, $\tau = 120$ ms) of the free DNA (green) and the $^{13}C/^{15}N$ filtered NOESY spectrum of the zf1-3/DNA complex (black).

tained by examining strips from 3D HNCO spectra (Grzesiek and Bax, 1992b), once backbone N and H^N shifts had been assigned. This procedure provided a nearly complete assignment of protein ^1H, ^{13}C and ^{15}N resonances (Table 2). Stereospecific β-proton assignments were obtained from analysis of 3D HNHB (Archer et al., 1991), HACAHB-COSY (Grzesiek et al., 1995) and ^{15}N-separated NOESY spectra.

Discontinuity in the HNCA- and HN(CO)CA-based backbone assignments occurred at three positions in the protein. Two were due to the presence of proline residues and one resulted from the extreme broadening of the backbone signals of His^{58} and His^{59}. Resonances within the two proline spin systems (Pro^{42} and Pro^{44}) in zf1-3 were assigned from 3D HCCH-correlated data and distinguished unambiguously by the presence of strong sequential $H^\alpha(i)$-$H^N(i+1)$ NOEs in ^{15}N-separated NOESY and $H^\beta(i-1)$-$H^\delta(i)$ NOEs in ^{13}C-separated NOESY spectra. These observations also confirm that both X-Pro amide bonds adopt the *trans* conformation. The backbone H^N and N resonances of His^{58} and His^{59} were too broad to be observed in the NMR spectra. The C^α resonance of His^{59} could be assigned based on correlations from Leu^{60} in the HN(CO)CA and CBCA(CO)NH spectra; however, the C^β resonance was not observed and the corresponding H^α and H^β cross peaks were absent from the HBHA(CBCACO)NH spectrum. Similarly, backbone amide assignments of His^{58} could not be obtained due to extreme broadening, and $C^\alpha H$, $C^\beta H$ and $C^{\delta 2}H$ resonances were obtained by the use of ambiguous restraints as described below. Protein resonance assignments are reported in Table 2.

The backbone N and H^N assignments obtained for zf1-3 in complex with DNA are shown in the 750 MHz ^{15}N HSQC spectrum of the complex at 310 K (Figure 1). Backbone N and H^N resonance assignments at 300 K can be found in the supplementary material. Figure 2 contains a summary of backbone chemical shift (Wishart and Sykes, 1994b), NOE and coupling constant data reflecting the secondary structural features of zf1-3 in complex with DNA. These NMR data are in good agreement with the solution structure, and the secondary structural elements are well defined (Foster et al., 1997; Wuttke et al., 1997).

Table 4. DNA ^{1}H shifts in the zf1-3/DNA complex, at 310 K

Nucleotide	H1′	H2′ H2″	H3′	H4′	H2/H5/H7	H6/H8	Others
T1	5.95	2.10,2.40	4.66	4.06	1.66	7.50	
T2	5.65	1.90,2.54	4.96	4.26	1.81	7.48	
G3	5.97	3.38,2.99	5.25	4.45		8.28	
G4	5.90	2.32,2.97	5.02	4.40		7.62	(H1) 12.77
A5	6.06	2.32,3.00	5.05	4.19	(H2) 7.73	7.98	
T6	5.77	1.89,2.39	5.03	4.26	0.99	6.87	(H3) 13.34
G7	6.05	2.70,3.03	5.06	4.09		7.94	(H1) 12.77
G8	5.82	2.53,2.96	5.13	4.30		7.55	(H1) 12.86
G9	5.55	2.29,2.18	4.87	4.42		7.56	(H1) 12.55
A 10	6.22	2.54,3.00	5.13	4.50	(H2) 7.46	8.23	
G11	5.53	2.64,2.77	5.04	4.41		7.84	(H1) 12.57
A12	6.33	2.73,3.00	5.04	4.51	(H2) 7.86	8.25	
C13	5.81	1.97,2.43	4.79	4.13	5.24	7.21	
C14	5.72	1.94,2.35	4.80	4.08	5.56	7.40	
G15	6.19	2.61,2.39	4.68	4.18		7.93	
C16	5.81	2.07,2.53	4.79	4.09	5.92	7.66	
G17	5.86	2.95,2.95	5.34	4.45		8.23	
G18	6.09	2.62,2.82	5.03	4.51		7.90	(H1) 12.97
T19	6.09	2.14,2.55	4.84	4.17	1.13	7.18	(H3) 13.52
C20	5.90	2.12,2.51	4.70	4.17	5.08	7.41	
T21	6.03	2.23,2.70	4.86	4.27	1.42	7.37	(H3) 13.66
C22	5.81	1.99,2.55	4.75	4.22	5.00	7.48	
C23	5.94	2.03,2.44	4.78	4.11	5.49	7.58	
C24	5.58	2.09,2.45	4.86	4.16	5.14	7.55	
A25	6.32	2.68,3.04	5.03	4.43		8.36	
T26	5.71	2.05,2.33	4.84	4.15	1.48	7.16	(H3) 13.63
C27	6.05	2.23,2.51	4.80	4.22	5.62	7.61	
C28	5.50	1.48,2.12	4.74	4.00	5.58	7.31	
A29	5.93	2.63,2.72	4.98	4.31	(H2) 7.78	8.12	
A30	6.24	2.63,2.40	4.69	4.20	(H2) 7.78	8.12	

DNA assignments

Resonance assignments of the non-exchangeable protons for the free DNA oligonucleotide (Table 3) were obtained at 750 MHz and at 310 K by standard homonuclear methods, employing the sequential assignment procedure for DNA (Wüthrich, 1986). Resonance assignments for DNA in complex with zf1-3 (Table 4) were obtained in a similar manner from 2D doubly ^{13}C/^{15}N-filtered NOESY (Figure 3), and 2D ^{13}C/^{15}N ω_2-filtered TOCSY spectra (Ikura and Bax, 1992; Burgering et al., 1993; Slijper et al., 1996). Imino proton assignments for the DNA in the complex were extracted from 2D jump-and-return NOESY spectra in 95:5 H_2O/D_2O. Resonance assignments were complete for H1′, H2′1, H2′2, H3′, H4′, H2, H5, H6, H7-methyl and H8 resonances (Tables 3 and 4) and formed the basis for our comparisons.

Ambiguous assignments

Conformational averaging of many DNA-contacting residues in the zf1-3/DNA complex (Foster et al., 1997) leads to broadening of resonances for these residues and the absence of important heteronuclear correlations for making resonance assignments. When resonance assignments could not be made unambiguously based exclusively on spectroscopic information (i.e., through-bond magnetization transfer), and yet clear intermolecular NOEs were observed in the ^{13}C-edited, ^{13}C/^{15}N-filtered NOESY (Lee et al., 1994), we employed ambiguous restraints (Nilges, 1995) as an unbiased approach for attempting to assign those

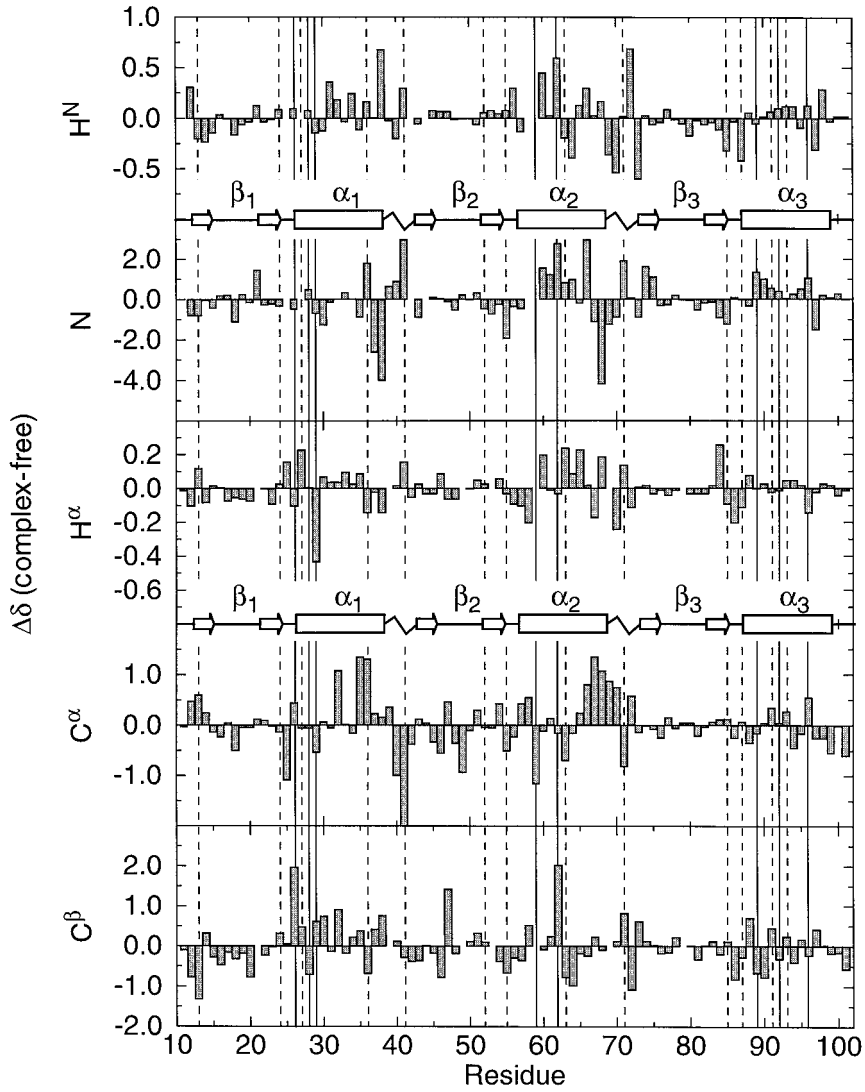

Figure 6. Changes in H^N, N, H^α, C^α and C^β chemical shifts of zf1-3 upon binding DNA. Dotted lines indicate residues that contact the phosphate backbone, solid lines indicate sites that contact bases.

resonances based on structural information. For example, using this approach, unambiguous assignment of NOEs in the $^{13}C/^{15}N$-filtered NOESY spectra to the 7-methyl protons of T4 and T21 allowed us to assign the $C^\delta H_2$ resonances of Arg^{62} and the $C^\alpha H$, $C^\beta H_2$ and $C^{\delta 2}H$ resonances of His^{58}, respectively. Both of these side-chains form intimate contacts with the DNA (Foster et al., 1997; Wuttke et al., 1997).

Chemical shift changes

Complexation of zf1-3 and its binding site induces dramatic changes in the chemical shifts and line shapes of signals in the NMR spectra of both molecules. An overlay of the ^{15}N HSQC spectra for the free and bound zf1-3 is shown in Figure 4, and the fingerprint regions (base to H2′1, H2′2) from 2D NOESY and 2D $^{13}C/^{15}N$-filtered NOESY of the free and bound DNA are overlaid in Figure 5.

Protein

Perturbations in the chemical shifts of the N, H^N, H^α, C^α, and C^β resonances for each residue in zf1-3 upon DNA binding are plotted in Figure 6. Protein residues that in the solution structures (Foster et al., 1997; Wuttke et al., 1997) were found to contact the DNA

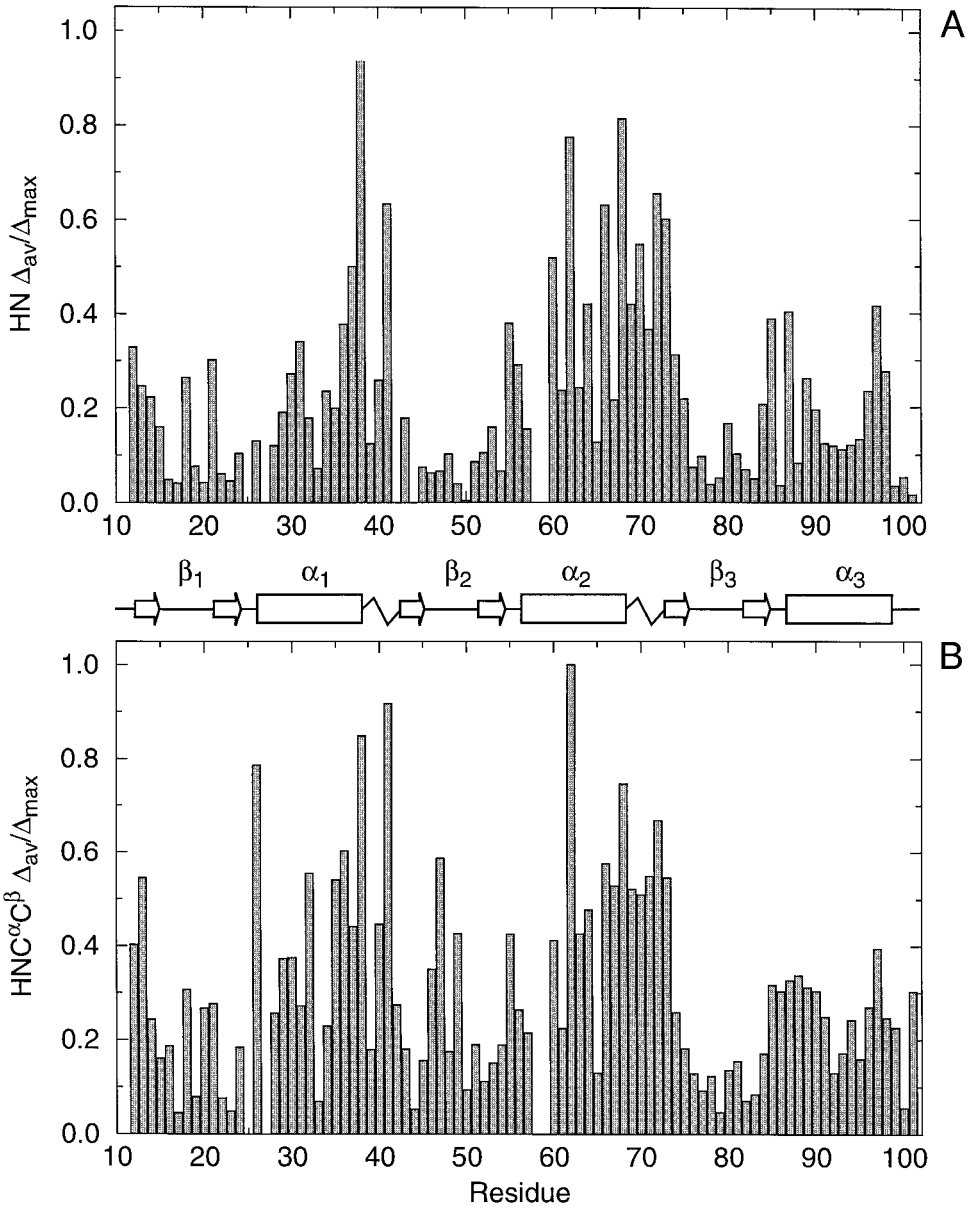

Figure 7. Normalized weighted average chemical shift differences (Δ_{av}/Δ_{max}) for zf1-3 upon DNA binding plotted against residue number for (A) amide proton and nitrogen resonances (Garrett et al., 1997), and (B) amide proton, nitrogen, C^{α} and $C\beta$ resonances (Grzesiek et al., 1996).

phosphate backbone are indicated by dotted lines, and those that interact with bases are indicated by solid lines. To determine which residues in zf1-3 exhibit significant chemical shift perturbations upon binding DNA, we calculated, for each residue, the normalized weighted average chemical shift differences for the backbone amide ^{1}H and ^{15}N resonances, $\Delta_{av}(NH)$, or the amide, $^{13}C^{\alpha}$ and $^{13}C^{\beta}$ resonances, $\Delta_{av}(NHC^{\alpha}C^{\beta})$ (Grzesiek et al., 1996; Garrett et al., 1997); these values are shown in Figure 7. To investigate the structural implications of these shift changes, we have color-coded the protein backbone as a function of the normalized chemical shift deviations, $\Delta_{av}/\Delta_{max}(NH)$ and $\Delta_{av}/\Delta_{max}(NHC^{\alpha}C^{\beta})$ (Figure 8). In addition, to assess whether side-chain resonances might be better indicators of recognition, we have investigated

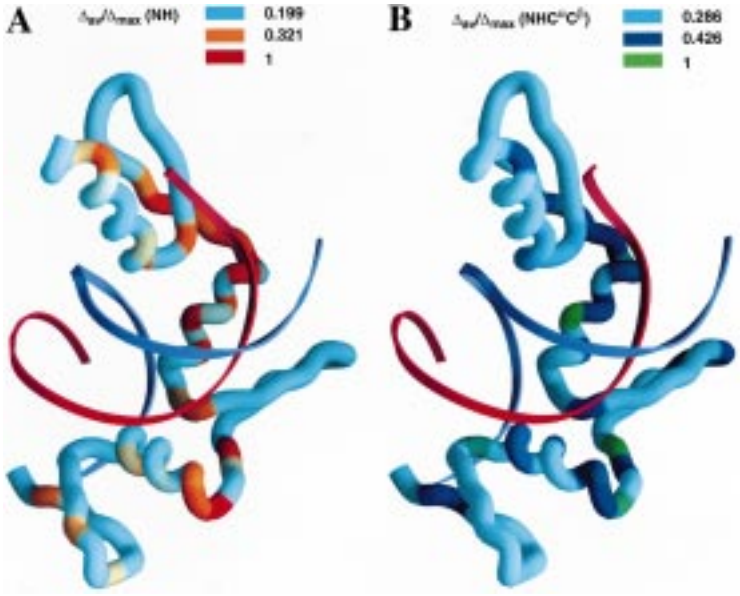

Figure 8. Normalized weighted average shift differences (A) Δ_{av}(HN), and (B) Δ_{av}(HNC$^{\alpha}$C$^{\beta}$) mapped onto a tube representation of the mean structure of zf1-3. The phosphate backbone of the DNA is drawn as two strands. The color ramps have been selected such that residues with Δ_{av} values below the trimmed mean (0.199 for HN and 0.286 for HNC$^{\alpha}$C$^{\beta}$) are colored cyan, with the midpoint of the color ramp (orange for HN and blue for HNC$^{\alpha}$C$^{\beta}$) selected at one standard deviation from the corresponding trimmed mean (trimmed mean plus rmsd, equals 0.321 for HN and 0.426 for HNC$^{\alpha}$C$^{\beta}$), and the end of the color ramp at unity (Δ_{max}).

chemical shift changes for a number of the side-chain resonances of zf1-3 (Table 5).

DNA

The differences in the chemical shifts of DNA protons free in solution and bound to zf1-3 are shown in Figure 9. To directly examine the structural implications of the chemical shift changes, we have mapped the magnitude (absolute value) of the ^{1}H chemical shift changes to the surface of the DNA molecule (Figure 10). As for the protein, we have also evaluated the weighted average chemical shift changes per nucleotide for the DNA (Figure 11).

Discussion

Chemical shift perturbations often accompany the binding of two biomolecules due to changes in the chemical environments of the atoms in the interface. Consequently, one goal of chemical shift analysis is to identify, in the absence of detailed structural information, the sites of local interactions between the two molecules. If the resonances that shift upon binding correspond to the residues directly involved in recognition, chemical shift changes can provide valuable insights into the structural basis for recognition, and should serve to guide design or screening efforts focused on the discovery of novel ligands. Notably, increased line widths due to intermediate time scale motions also are common in biomolecular complexes (Qian et al., 1993; Kay et al., 1996; Brodsky and Williamson, 1997; Foster et al., 1997). This phenomenon underscores the importance of mobility in mediating recognition but presents the vexing problem that those protein residues of greatest interest from the standpoint of detailing the structural basis for molecular recognition are the most challenging to study.

The existence of a high-resolution structure of the zf1-3/DNA complex (Foster et al., 1997; Wuttke et al., 1997), and the availability of resonance assignments of the free zf1-3 protein (Liao et al., 1994) and those reported here for the DNA-bound zf1-3 protein and the free and complexed DNA binding site, enable us to analyze the correlation between chemical shift perturbations and intermolecular contacts. We examined whether those residues on the protein and DNA that exhibit the largest chemical shift deviations are those involved directly in mediating molecular recognition.

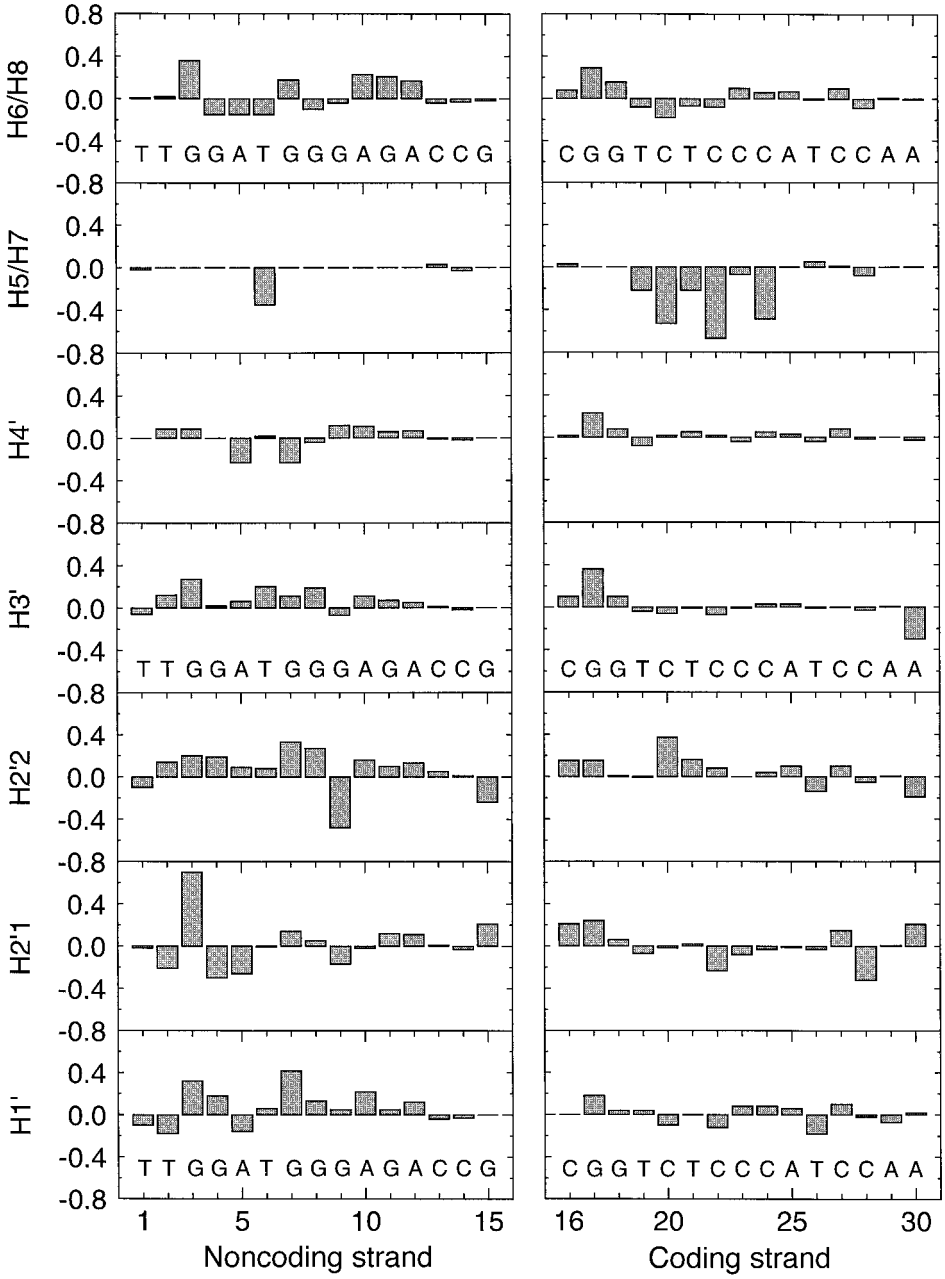

Figure 9. Plot of chemical shift changes upon protein binding against nucleotide for assigned DNA protons.

Protein shifts

The pattern of chemical shift changes for individual protein H^N, N, H^α, C^α and C^β resonances upon DNA binding (Figure 6) is not well correlated with DNA contacts observed in the solution structure of the complex (Foster et al., 1997; Wuttke et al., 1997). Indeed, the largest perturbations of the backbone H^N resonances are seen for residues that do not contact DNA: the H^N resonances of Thr^{38}, Glu^{72}, Phe^{73} are each shifted by more than 0.5 ppm on complex formation. Nevertheless, significant shift differences are seen for the H^N resonances of some DNA-contacting residues, e.g., Arg^{62}, which makes a specific base contact, and Lys^{41}, Thr^{85} and Lys^{87}, each of which contact the DNA phosphate backbone. Similarly, individual N,

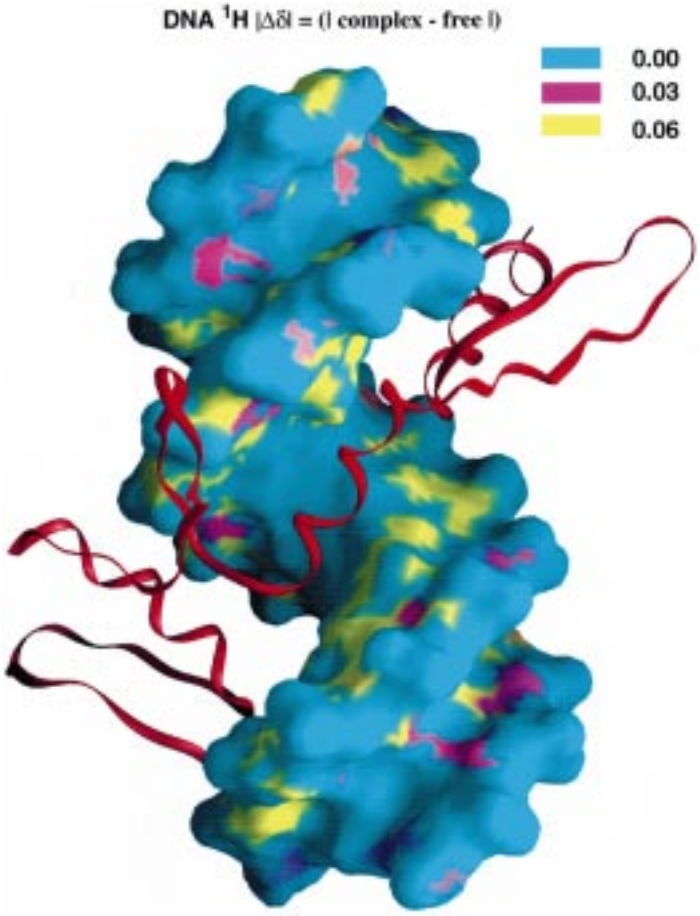

Figure 10. Surface representation of the DNA, color coded according to chemical shift deviations.

H^{α}, C^{α} and C^{β} shift perturbations for each residue are not well correlated with each other or with the observed intermolecular contacts.

Residues whose resonances are affected by binding may be more readily identified by considering the weighted average chemical shift change for each residue (Grzesiek et al., 1996; Garrett et al., 1997). The backbone amide ^{1}H and ^{15}N shifts are often used as diagnostic probes because these resonances are generally well resolved for folded proteins. Another advantage of considering only the amide signals is that once the resonances have been assigned, binding studies can be performed with relatively inexpensive material uniformly labeled only with ^{15}N. Of course, H^{N} and N shifts are not sensitive to the same environmental and structural parameters as the H^{α}, C^{α}, and C^{β} shifts (Wishart et al., 1992; Wishart and Sykes, 1994a,b), which can generally be readily assigned for doubly labeled ($^{13}C/^{15}N$) proteins, providing valuable complementary information when available.

The H^{N} and N weighted average shift differences reveal that significant chemical shift deviations map almost exclusively to the ends of the helices and the linker regions between the domains (Figures 7A and 8A). If one considers the C^{α} and C^{β} shift differences for zf1-3 in addition to H^{N} and N, a similar pattern holds, but the shift perturbations are somewhat more evenly distributed throughout the protein (Figures 7B and 8B). These regions of the protein are not implicated in sequence specificity (with the exception of Arg^{96}, which does contact a DNA base), but rather are probably reflecting substantial conformational and dynamical changes that take place in these regions of the protein upon DNA binding (Foster et al., 1997; Wuttke et al., 1997).

In particular, the ends of the helices and the linkers are intimately implicated in the formation of contact

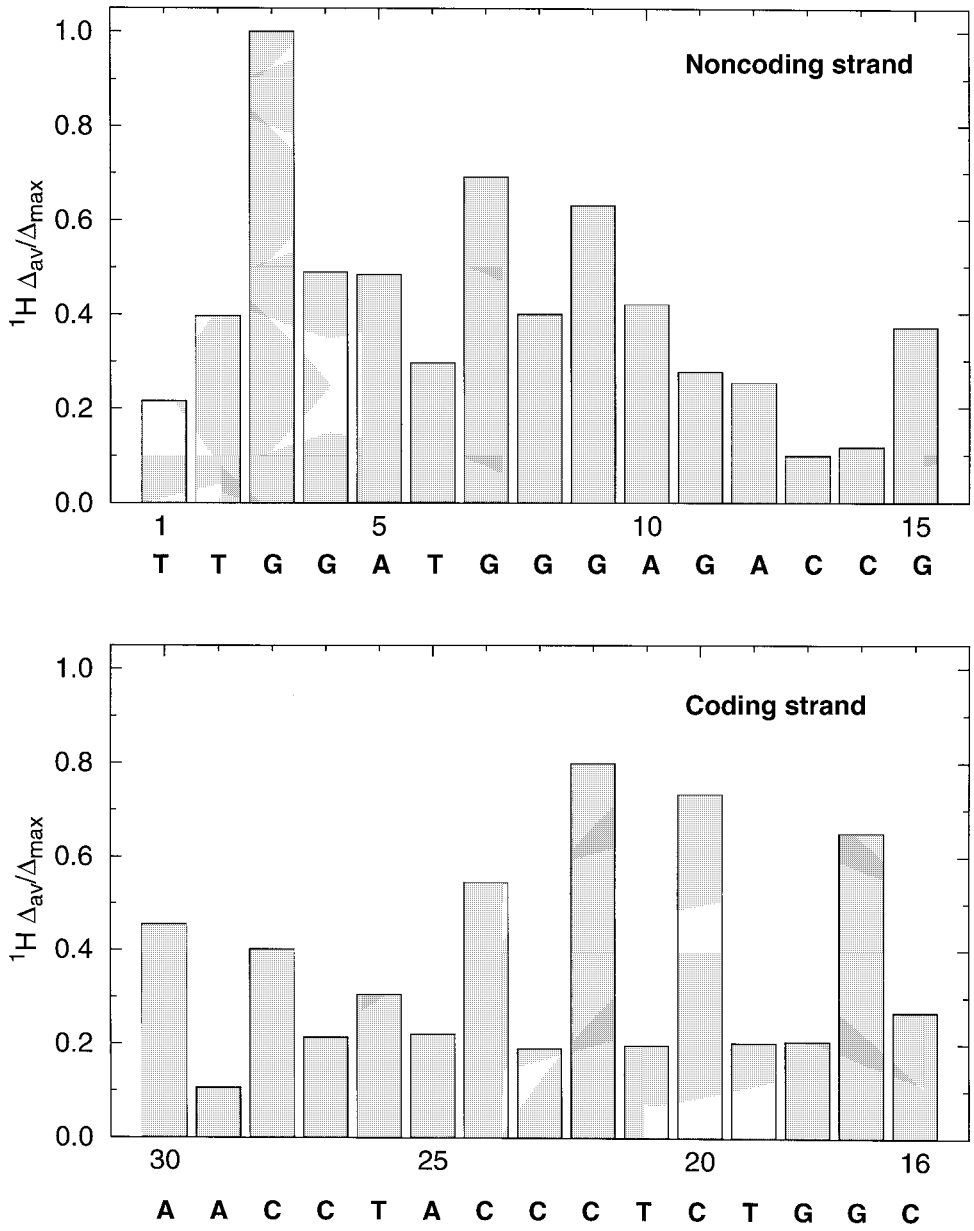

Figure 11. Weighted averaged DNA 1H shift differences for the top (1–15) and bottom (16–30) strands. Δ_{av} is the RMS deviation per residue of all assigned protons (ppm).

surfaces between adjacent zinc finger domains. These are flexible in the free protein (Brüschweiler et al., 1995), but become rigid and pack onto the rest of the protein upon binding DNA (Foster et al., 1997; Wuttke et al., 1997). In fact, the regions in which we observe the most significant chemical shift differences at the backbone level agree well with the regions of the protein that adopt more ordered structures in complex with DNA relative to the free protein (Foster et al., 1997). These observations imply that relying exclusively upon ^{1}H and ^{15}N correlated spectra to assay for binding and to map intermolecular binding surfaces provides an incomplete analysis and, in cases where binding has induced significant conformational changes, these interpretations may lead to incorrect assumptions about the nature of the interactions.

Side-chains play a dominant role in molecular recognition by proteins. Unfortunately, monitoring

Table 5. zf1-3 side-chain shift changes (complex – free)

Residue	Interface	Position	$\Delta\delta_x$	$\Delta\delta_H$	Δ_{av}[a]
Lys^{26}	DNA	C^{β}	2.1	0.27	0.77
Lys^{26}	DNA	C^{γ}	1.0	0.11	0.36
Trp^{28}	DNA	N^{ϵ}	5.5	0.39	0.83
Trp^{28}	DNA	$C^{\epsilon 3}$	−2.4	0.20	0.86
Lys^{29}	DNA	C^{β}	0.8	−0.22	0.32
Lys^{29}	DNA	C^{γ}	0.3	−0.53	0.39
Ala^{32}	Protein	C^{β}	1.0	0.12	0.36
Thr^{55}	Protein	Cβ	−0.5	0.08	0.19
Thr^{55}	Protein	Cγ	0.5	0.05	0.18
Arg^{62}	DNA	C^{δ}	1.9	−0.21	0.69
Thr^{85}	Protein	C^{γ}	1.4	0.14	0.50
Thr^{86}	Protein	C^{γ}	−1.0	−0.36	0.44
Arg^{96}	DNA	C^{δ}	1.0	0.12	0.36

Note: Δ_{max} for amide N and H^N is 0.73; Δ_{max} for $HNC^{\alpha}C^{\beta}$ is 2.0.

a Δ_{av} was calculated as $[(\Delta H)^2 + (\Delta C/2)^2)2]^{1/2}$ for $^1H/^{13}C$ pairs and $[(\Delta H)^2 + (\Delta N/5)^2)/2]^{1/2}$ for $^1H/^{15}N$ pairs.

the chemical shifts of side-chains in uniformly labeled proteins is not generally practical as a diagnostic method for monitoring interactions, largely because of severe overlap and the relative difficulty in obtaining assignments of side-chain resonances. In order to assess whether side-chain chemical shift perturbations accurately reflect the nature of the intermolecular interaction, we have investigated chemical shift changes for a number of the side-chain resonances of zf1-3 that are in either protein–DNA or protein–protein interfaces (Table 5). In fact, the largest ^1H chemical shift deviation upon DNA binding is seen for the $N^{\epsilon 1}$ indole proton of Trp^{28}, in finger 1. Upon DNA binding this resonance shifts downfield 0.68 ppm in the ^1H dimension (from 10.31 to 10.99, at 300 K), and the ^{15}N frequency by 0.7 ppm (Figure 4). This perturbation likely reflects the electronic consequences of hydrogen bonding to the O6 atom of G11 in the complex. However, the data in Table 5 reveal that, like the backbone resonances, side-chain resonances appear to be at least as affected by DNA binding as by protein–protein packing and changes in dynamics.

DNA

In the solution structure, the DNA adopts a conformation very close to B-form. The fingers of zf1-3 bind in the major groove making base contacts to nucleotides G3–G11 on the noncoding strand, and nucleotides G17–T19 and T21, C24 and T26 on the coding strand (Wuttke et al., 1997). The chemical shift changes of base H6, H8, H5 and H7-methyl protons in the major groove *do* appear to be well correlated with the intermolecular contact region on the DNA. For example, the H8 proton of G3 is shifted by almost 0.4 ppm, reflecting the intimacy of the contact from finger 3 of zf1-3 (Phe^{97} packs against the backbone ribose and Arg^{96} contacts the N7).

On the noncoding strand, significant shift perturbations are observed for H6/H8 proton resonances from G3 to A12, where finger 1 then crosses the major groove to interact with the coding strand. The exception is the H8 proton of G9, which is not significantly perturbed; interestingly, the nature of this base does not appear to be important for binding by TFIIIA (Veldhoen et al., 1994).

On the coding strand, the H8 protons of G17 and G18 are shifted, reflecting binding of finger 1 in this region (Wuttke et al., 1997). The H5 and H7 methyl protons of T19–C24 are also shifted (as much as 0.6 ppm for C22 H5), undoubtedly a consequence of interactions of the protein with both strands in this region of the DNA. The H6/H8 and H5/H7 protons are not significantly perturbed past C24, where the helix of finger 3 diverges from this strand.

The pattern of chemical shift changes in the sugar-phosphate backbone is less well correlated with binding interactions. Nevertheless, there are some notable perturbations that correlate with protein–DNA contacts: G3 H2′ shifts > 0.6 ppm due to the interaction of finger 3 with this base, G17 H3′ and H4′ are probably reflecting a phosphate contact from Tyr^{13}, and the H2′1 of G9 and H2′2 of C20 shifts likely reflect protein contacts.

Clearly, many of the DNA protons that exhibit significant shift perturbations upon protein binding map to regions of the surface that directly contact the protein. However, there are also several examples of large perturbations that do not result from direct protein–DNA contacts. While using the weighted average shift change per nucleotide to analyze the intermolecular contacts lacks the structural detail of a proton-by-proton analysis, we can see that the primary perturbations in the proton chemical shifts closely follow the binding surface of zf1-3 (Figures 10 and 11), contacting the noncoding strand at the 5′ and middle of the binding site (nucleotides 3–12) and the coding strand at the 3′ end of the binding site. Notably, this figure exhibits striking similarity to a plot of intermolecular NOEs per nucleotide (Wuttke et al., 1997).

Conclusions

We have found changes in DNA base-proton chemical shifts to be reasonably good markers of intermolecular contacts in the zf1-3/DNA complex, in a case where the structure of the DNA is not significantly distorted from its free solution conformation. However, our analysis of the chemical shift changes of the protein upon binding indicates that relying on backbone chemical shift changes to identify protein residues that are involved in specific intermolecular interactions can be misleading when significant structural and dynamic changes accompany binding. Many proteins that bind to and recognize other molecules undergo conformational transitions as a part of the recognition process. Indeed, possessing flexible regions enables fine control over stability of a molecular complex such that specificity and affinity are appropriate for biological function. This property may limit the applicability of chemical shift analysis in the study of biomolecular interactions; like mutagenesis footprinting and other methods that provide indirect structural information, chemical shift changes must be interpreted carefully.

Acknowledgements

The authors acknowledge J. Cavanagh and M. Rance for assistance with NMR experiments, L. Xiang and G.P. Gippert for semiautomated NMR assignment tools, D. Case for implementation of ambiguous restraints in AMBER, J. Love, D. Casimiro, D. Sem, S. Holmbeck and J. Dyson for helpful discussions, and Tripos Inc. and MSI Inc. for providing NMR processing and analysis software. M.P.F. was supported by a postdoctoral fellowship from the American Cancer Society, D.S.W. by an NSF postdoctoral fellowship, I.R. by a fellowship from the Jane Coffin Childs Research Foundation, and W.J. by a Studienstiftung des Deutschen Volkes. This work was supported by Grant GM36643 from the National Institutes of Health.

References

Archer, S.J., Ikura, M., Torchia, D.A. and Bax, A. (1991) *J. Magn. Reson.*, **95**, 636–641.

Bax, A. and Subramanian, S. (1986) *J. Magn. Reson.*, **67**, 565–569.

Bax, A., Clore, G.M., Driscoll, P.C., Gronenborn, A.M., Ikura, M. and Kay, L.E. (1990a) *J. Magn. Reson.*, **87**, 620–627.

Bax, A., Clore, G.M. and Gronenborn, A.M. (1990b) *J. Magn. Reson.* **88**, 425–431.

Bax, A., Ikura, M., Kay, L.E., Torchia, D.A. and Tschudin, R. (1990c) *J. Magn. Reson.*, **86**, 304–318.

Bax, A., Ikura, M., Kay, L.E. and Zhu, G. (1991) *J. Magn. Reson.*, **91**, 174–178.

Bax, A. and Pochapsky, S. (1992) *J. Magn. Reson.*, **99**, 638–643.

Berg, J.M. (1990) *Annu. Rev. Biophys. Biophys. Chem.*, **19**, 405–421.

Bodenhausen, G. and Ruben, D.G. (1980) *Chem. Phys. Lett.*, **69**, 185–189.

Brodsky, A.S. and Williamson, J.R. (1997) *J. Mol. Biol.*, **267**, 624–639.

Brüschweiler, R., Liao, X. and Wright, P.E. (1995) *Science*, **268**, 886–889.

Burgering, M., Boelens, R. and Kaptein, R. (1993) *J. Biomol. NMR*, **3**, 709–714.

Cavanagh, J. and Rance, M. (1993) *Annu. Rep. NMR Spectrosc.*, **27**, 1–58.

Chen, Y., Reizer, J., Saier, Jr., M.H., Fairbrother, W.J. and Wright, P.E. (1993) *Biochemistry*, **32**, 32–37.

Clemens, K.R., Liao, X., Wolf, V., Wright, P.E. and Gottesfeld, J.M. (1992) *Proc. Natl. Acad. Sci. USA*, **89**, 10822–10826.

Delaglio, F., Grzesiek, S., Vuister, G.W., Guang, Z., Pfeifer, J. and Bax, A. (1995) *J. Biomol. NMR*, **6**, 277–293.

Elrod-Erickson, M., Rould, M.A., Nekludova, L. and Pabo, C.O. (1996) *Structure*, **4**, 1171–1180.

Emerson, S.D., Madison, V.S., Palermo, R.E., Waugh, D.S., Scheffler, J.E., Tsao, K.-L., Kiefer, S.E., Liu, S.P. and Fry, D.C. (1995) *Biochemistry*, **34**, 6911–6918.

Engelke, D.R., Ng, S.-Y., Shastry, B.S. and Roeder, R.G. (1980) *Cell*, **19**, 717–728.

Fairall, L., Rhodes, D. and Klug, A. (1986) *J. Mol. Biol.*, **192**, 577–591.

Fairall, L., Schwabe, J.W.R., Chapman, L., Finch, J.T. and Rhodes, D. (1993) *Nature*, **366**, 483–487.

Foster, M.P., Wuttke, D.S., Case, D.A., Gottesfeld, J.M. and Wright, P.E. (1997) *Nat. Struct. Biol.*, **4**, 605–608.

Garrett, D.S., Seok, Y.-J., Peterkofsky, P., Clore, G.M. and Gronenborn, A.M. (1997) *Biochemistry*, **26**, 4393–4398.

Ginsberg, A.M., King, B.O. and Roeder, R.G. (1984) *Cell*, **39**, 479–489.

Gronenborn, A.M. and Clore, G.M. (1993) *J. Mol. Biol.*, **233**, 331–335.

Grzesiek, S. and Bax, A. (1992a) *J. Am. Chem. Soc.*, **114**, 6291–6293.

Grzesiek, S. and Bax, A. (1992b) *J. Magn. Reson.*, **99**, 201–207.

Grzesiek, S. and Bax, A. (1993a) *J. Biomol. NMR*, **3**, 185–204.

Grzesiek, S. and Bax, A. (1993b) *J. Am. Chem. Soc.*, **115**, 12593–12594.

Grzesiek, S., Kuboniwa, H., Hinck, A.P. and Bax, A. (1995) *J. Am. Chem. Soc.*, **117**, 5312–5315.

Grzesiek, S., Bax, A., Clore, G.M., Gronenborn, A.M., Hu, J.S., Kaufman, J., Palmer, I., Stahl, S.J. and Wingfield, P.T. (1996) *Nat. Struct. Biol.*, **3**, 340–345.

Guddat, U., Bakken, A.H. and Pieler, T. (1990) *Cell*, **60**, 619–628.

Hajduk, P.J., Sheppard, G., Nettesheim, D.G., Olejniczak, E.T., Shuker, S.B., Meadows, R.P., Steinman, D.H., Carrera Jr., G.M., Marcotte, P.A., Severin, J., Walter, K., Smith, H., Gubbins, E., Simmer, R., Holzman, T.F., Morgan, D.W., Davidsen, S.K., Summers, J.B. and Fesik, S.W. (1997) *J. Am. Chem. Soc.*, **119**, 5818–5827.

Hayes, J.J. and Tullius, T.D. (1992) *J. Mol. Biol.*, **227**, 407–417.

Honda, B.M. and Roeder, R.G. (1980) *Cell*, **22**, 119–126.

Houbaviy, H.B., Usheva, A., Shenk, T. and Burley, S.K. (1996) *Proc. Natl. Acad. Sci. USA*, **93**, 13577–13582.

Ikura, M. and Bax, A. (1992) *J. Am. Chem. Soc.*, **114**, 2433–2440.
Kay, L.E., Marion, D. and Bax, A. (1989) *J. Magn. Reson.*, **84**, 72–84.
Kay, L.E., Ikura, M. and Bax, A. (1990) *J. Am. Chem. Soc.*, **112**, 888–889.
Kay, L.E., Keifer, P. and Saarinen, T. (1992) *J. Am. Chem. Soc.*, **114**, 10663–10665.
Kay, L.E., Xu, G.Y. and Yamazaki, T. (1994) *J. Magn. Reson.*, **A109**, 129–133.
Kay, L.E. (1995) *Curr. Opin. Struct. Biol.*, **5**, 674–681.
Kay, L.E., Muhandiram, D.R., Farrow, N.A., Aubin, Y. and Forman-Kay, J.D. (1996) *Biochemistry*, **35**, 361–368.
Kim, C.A. and Berg, J.M. (1996) *Nat. Struct. Biol.*, **3**, 940–945.
Lee, W., Revington, M.J., Arrowsmith, C. and Kay, L.E. (1994) *FEBS Lett.*, **350**, 87–90.
Liao, X., Clemens, K.R., Tennant, L., Wright, P.E. and Gottesfeld, J.M. (1992) *J. Mol. Biol.*, **223**, 857–871.
Liao, X., Clemens, K.R., Cavanagh, J., Tennant, L. and Wright, P.E. (1994) *J. Biomol. NMR*, **4**, 433–454.
Live, D.H., Davis, D.G., Agosta, W.C. and Cowburn, D. (1984) *J. Am. Chem. Soc.*, **106**, 6104–6105.
Marion, D. and Bax, A. (1988) *J. Magn. Reson.*, **79**, 352–356.
Messerle, B.A., Wider, G., Otting, G., Weber, C. and Wüthrich, K. (1989) *J. Magn. Reson.*, **85**, 608–613.
Miller, J., McLachlan, A.D. and Klug, A. (1985) *EMBO J.*, **4**, 1609–1614.
Muhandiram, D.R. and Kay, L.E. (1994) *J. Magn. Reson.*, **B103**, 203–216.
Nicholls, A., Sharp, K.A. and Honig, B. (1991) *Proteins*, **11**, 281–296.
Nilges, M. (1995) *J. Mol. Biol.*, **245**, 645–660.
Orbons, L.P., van der Marel, G.A., van Boom, J.H. and Altona, C. (1987) *Eur. J. Biochem.*, **170**, 225–239.
Otting, G. and Wüthrich, K. (1990) *Q. Rev. Biophys.*, **23**, 39–96.
Palmer, A.G., Cavanagh, J., Wright, P.E. and Rance, M. (1991) *J. Magn. Reson.*, **93**, 151–170.
Pavletich, N.P. and Pabo, C.O. (1991) *Science*, **252**, 809–817.
Pavletich, N.P. and Pabo, C.O. (1993) *Science*, **261**, 1701–1707.
Pelham, H.R. and Brown, D.D. (1980) *Proc. Natl. Acad. Sci. USA*, **77**, 4170–4174.
Pieler, T. and Theunissen, O. (1993) *Trends Biochem. Sci.*, **18**, 226–230.
Qian, Y.Q., Otting, G., Billeter, M., Muller, M., Gehring, W. and Wüthrich, K. (1993) *J. Mol. Biol.*, **234**, 1070–1083.
Scmiedeskamp, M., Rajagopal, P. and Klevitt, R.E. (1997) *Protein Sci.*, **6**, 1835–1848.
Shuker, S.B., Hajduk, P.J., Meadows, R.P. and Fesik, S.W. (1996) *Science*, **274**, 1531–1534.
Slijper, M., Kaptein, R. and Boelens, R. (1996) *J. Magn. Reson.*, **B111**, 199–203.
Spolar, R.S. and Record, Jr., M.T., (1994) *Science*, **263**, 777–784.
States, D.J., Haberkorn, R. and Ruben, D. (1982) *J. Magn. Reson.*, **48**, 286–292.
Van Nuland, N.A.J., Kroon, G.J.A., Dijkstra, K., Wolters, G.K., Scheek, R.M. and Robillard, G.T. (1993) *FEBS Lett.*, **315**, 11–15.
Van Nuland, N.A.J., Boelens, R., Scheek, R.M. and Robillard, G.T. (1995) *J. Mol. Biol.*, **246**, 180–193.
Veldhoen, N., You, Q., Setzer, D.R. and Romaniuk, P.J. (1994) *Biochemistry*, **33**, 7568–7575.
Vuister, G.W. and Bax, A. (1992) *J. Magn. Reson.*, **98**, 428–435.
Vuister, G.W. and Bax, A. (1993) *J. Am. Chem. Soc.*, **115**, 7772–7777.
Wishart, D.S., Sykes, B.D. and Richards, F.M. (1992) *Biochemistry*, **31**, 1647–1651.
Wishart, D.S. and Sykes, B.D. (1994a) *Methods Enzymol.*, **239**, 363–392.
Wishart, D.S. and Sykes, B.D. (1994b) *J. Biomol. NMR*, **4**, 171–180.
Wishart, D.S., Bigam, C.G., Yao, J., Abildgaard, F., Dyson, H.J., Oldfield, E., Markley, J.L. and Sykes, B.D. (1995) *J. Biomol. NMR*, **6**, 135–140.
Wong, I. and Lohman, T.M. (1995) *Methods Enzymol.*, **259**, 95–127.
Wüttrich, K. (1986) *NMR of Proteins and Nucleic Acids*, Wiley, New York, NY.
Wuttke, D.S., Foster, M.P., Case, D.A. and Wright, P.E. (1997) *J. Mol. Biol.*, **273**, 173–206.
Zhu, G. and Bax, A. (1992) *J. Magn. Reson.*, **98**, 192–199.